LIMNOLOGY and OCEANOGRAPHY

ASLO

Limnol. Oceanogr. 9999, 2020, 1–17

doi: 10.1002/lno.11465

Relative importance of top-down vs. bottom-up control of lake phytoplankton vertical distributions varies among fluorescence-based spectral groups

Mary E. Lofton [1]*, **Taylor H. Leach** [2], **Beatrix E. Beisner** [3], **Cayelan C. Carey** [1]

[1]Department of Biological Sciences, Virginia Tech, Blacksburg, Virginia
[2]Department of Biology, Miami University, Miami, Ohio
[3]Department of Biological Sciences and Groupe de recherche interuniversitaire en limnologie (GRIL), University of Québec at Montréal, Montréal, QC, Canada

Abstract

The relative importance of top-down vs. bottom-up control of phytoplankton biomass in aquatic ecosystems has been long debated and studied. However, few studies have considered the relative importance of top-down vs. bottom-up control on phytoplankton vertical distributions and characteristics of deep chlorophyll maxima (DCMs), and fewer still have investigated the importance of these drivers for multiple phytoplankton groups. We examined depth profiles of four phytoplankton spectral groups and a suite of top-down (zooplankton) and bottom-up (nutrients, temperature, and light) drivers from 51 north temperate lakes varying on gradients of size, trophic state, light availability, and thermal stratification. We used regression trees to identify the most important drivers of different vertical distribution metrics for each phytoplankton spectral group. The relative importance of top-down vs. bottom-up control varied across spectral groups and was related to the characteristics of the dominant taxa within each spectral group, as assessed by microscope counts. Zooplankton biomass was the most important driver of brown algae vertical distributions, likely because this group contained highly edible taxa (primarily chrysophytes), while thermal stratification predicted vertical distributions of buoyancy-regulating cyanobacteria. Our work highlights the importance of examining phytoplankton community composition to improve understanding of DCM characteristics and top-down vs. bottom-up control of phytoplankton in aquatic systems.

The relative importance of top-down vs. bottom-up control of phytoplankton biomass in aquatic ecosystems has been the subject of much research (Taylor et al. 2015 and references therein), with substantial evidence supporting the significance of both processes (Benndorf et al. 2002; Ellis et al. 2011; Bunnell et al. 2014). To date, most research considering top-down vs. bottom-up control has considered the effect of these controls on the *total biomass* of phytoplankton (Jeppesen et al. 2003; Sawatzky et al. 2006; Bunnell et al. 2014). However, it is well-recognized that the spatial distribution of phytoplankton biomass is highly structured across depth in stratified lakes, with aggregations often occurring in deep chlorophyll maxima (DCM) (Fee 1976; Abbott et al. 1984; Hamilton et al. 2010; Latasa et al. 2017; Leach et al. 2018). These subsurface maxima are widespread across both marine and freshwater ecosystems and have been the focus of much research (Durham and Stocker 2011; Cullen 2015 and references therein). Nonetheless, we still have very little understanding of the relative importance of top-down vs. bottom-up controls in determining the *vertical distribution* of different phytoplankton groups in lakes.

The depth and magnitude of DCMs may be driven by multiple physical, chemical, or biological factors, as DCMs can exist due to phytoplankton migration, growth, settling, or entrainment (Moll et al. 1984; Arvola et al. 1992; Durham and Stocker 2011). DCM depth may be determined by light attenuation, in which water columns with greater light penetration display deeper, broader DCMs (Varela et al. 1994; Hamilton et al. 2010; Leach et al. 2018), or by a combination of light attenuation and nutrients, in which phytoplankton select a depth to optimize both down-welling light and greater nutrient availability in hypolimnetic waters (Klausmeier and Litchman 2001; Karpowicz and Ejsmont-Karabin 2017; Hamre et al. 2018). Motile or buoyant phytoplankton will migrate to take advantage of these gradients of light, nutrients, or temperature and develop DCMs in layers with optimal resources (Moll et al. 1984;

*Correspondence: melofton@vt.edu

Additional Supporting Information may be found in the online version of this article.

Camacho et al. 2001; Sengupta et al. 2017). Conversely, in some conditions, DCMs may exist because senescent phytoplankton settle to a depth of neutral buoyancy or because phytoplankton are entrained via shear-induced mixing or interflows (Alldredge et al. 2002; Cullen 2015; Lewis et al. 2017). Biotic factors may also alter phytoplankton vertical structure, such as when zooplankton grazing mediates the magnitude and depth of the DCM or causes shifts in community structure due to preferential grazing (Lynch and Shapiro 1981; Arvola et al. 1992; Pilati and Wurtsbaugh 2003; Moeller et al. 2019). Alternatively, DCMs may exist due to niche differentiation among phytoplankton taxa in heterogeneous environmental conditions. For example, low-light tolerant taxa such as *Planktothrix* may either persist at the surface in well-mixed, eutrophic conditions or form a DCM in the shaded, deep layer under dominant surface-dwelling taxa in thermally stratified conditions (Yoshiyama et al. 2009; Ryabov and Blasius 2014). Notably, the currently identified ensemble of potential drivers of DCM depth and biomass include both bottom-up (light, nutrients, and thermal stratification) and top-down (zooplankton) controls, making DCMs especially interesting for examining the relative importance of these controls on the spatial distribution of organisms.

The majority of previous studies of DCMs examined only the vertical distributions of total phytoplankton biomass or of a single taxon (Christensen et al. 1995; Jeppesen et al. 2003; Kononen et al. 2003; Hamilton et al. 2010; Hamre et al. 2018; Leach et al. 2018), which could in part explain why there are so many different hypotheses and explanations for different DCM characteristics. Examination of total biomass obscures differences in the relative importance of top-down and bottom-up controls for different phytoplankton taxa. For example, the vertical distribution of diatoms, chrysophytes, and cryptophytes, which are highly nutritious and preferentially grazed by zooplankton, may be more driven by top-down control than inedible cyanobacteria (Brett et al. 2000, 2006), although cyanobacteria may also experience indirect top-down effects as their abundance increases due to zooplankton grazing down more edible taxa (Lynch and Shapiro 1981; Holm et al. 1983). In contrast, the vertical distribution of taxa that can control their motility or buoyancy in the water column, such as cyanobacteria with gas vesicles and green algae, dinoflagellates, cryptophytes, chrysophytes, and euglenoids with flagella, may be more driven by pH or bottom-up resource gradients of light, nutrients, or CO_2 (Shapiro 1973; Oliver 1994; Clegg et al. 2004, 2007; deNoyelles Jr et al. 2016). Thermal stratification can act as a physical control affecting migration strategy or settling location of phytoplankton in the water column, potentially allowing motile taxa to take advantage of well-stratified water columns by migrating to or maintaining buoyancy at a layer with optimal resources (Alldredge et al. 2002; Sengupta et al. 2017). Thus, it is likely that vertical distributions of different phytoplankton respond differently to top-down and bottom-up controls depending on their functional traits.

The few studies that have considered the vertical distribution of multiple phytoplankton groups find that different taxa can disperse and exhibit multiple, distinct DCMs (Barbiero and McNair 1996; Longhi and Beisner 2009; Selmeczy et al. 2016; Latasa et al. 2017). The degree of aggregation vs. segregation in the vertical distribution of different phytoplankton groups can be quantified by a spatial overlap statistic that characterizes the proportion of phytoplankton vertical profiles that co-occur across depth (Beisner and Longhi 2013). Low spatial overlap indicates vertical segregation of phytoplankton taxa into discrete, separate layers and high spatial overlap indicates aggregation of taxa into a single region of the water column (Beisner and Longhi 2013). Low spatial overlap among taxa may result from limitation by different resources; e.g., light-limited taxa are more likely to remain in the shallower region of the water column while low-light tolerant, nutrient-limited taxa will inhabit deeper waters (Longhi and Beisner 2009; Selmeczy et al. 2016). Beisner and Longhi (2013) found that strong thermal stratification, low light attenuation, and oligotrophic conditions promoted high spatial overlap of phytoplankton groups. However, we are unaware of any work explicitly considering top-down vs. bottom-up control of the vertical distributions of multiple phytoplankton groups as mediated by the functional traits of the dominant taxa observed in those communities.

The development of new multi-wavelength fluorescence sensors has the potential to advance our understanding of how different environmental variables affect vertical distributions of multiple phytoplankton groups (Beutler et al. 2002; Gregor and Maršálek 2004; Ghadouani and Smith 2005; Catherine et al. 2012; Kring et al. 2014). Historically, there has been a tradeoff in methods between optimizing the spatial and taxonomic resolution of phytoplankton vertical profiles: chlorophyll *a* (Chl *a*) sensors provide high-resolution vertical profiles but no taxonomic resolution, while microscope counts provide high taxonomic resolution but are often prohibitively labor- and cost-intensive for obtaining high spatial resolution (Catherine et al. 2012). Within the past two decades, new multi-wavelength fluorescence sensor technology has enabled a compromise between these two alternatives, providing both high-resolution vertical profiles and broad taxonomic information determined by assigning phytoplankton to "spectral groups" based on the known pigment fluorescence signature of different taxa (Beutler et al. 2002). While not as resolved taxonomically as species-level microscope counts, multi-wavelength fluorescence sensors provide a relatively cost-effective, portable alternative for measuring high-resolution vertical profiles of multiple phytoplankton groups across many lakes (Catherine et al. 2012).

We used a multi-wavelength fluorescence sensor to examine the relative importance of top-down and bottom-up controls on vertical distribution and DCMs of four phytoplankton spectral groups across 51 north temperate lakes spanning gradients of size, trophic state, light availability, and thermal stratification. We further verified the taxa represented by each of these spectral groups in our study lakes via microscope

counts of phytoplankton from vertical tows across the photic zone of each lake. We note that spectral groups may be comprised of taxa with a range of functional traits, and thus we formulated hypotheses that were as specific as possible given the limitations of what can be measured with a spectral probe and the data available to validate these measurements.

Based on the range of taxa encompassed within spectral groups, we predicted that the relative importance of top-down vs. bottom-up control on vertical distributions would vary among spectral groups. Specifically, we hypothesized that the vertical distribution of phytoplankton groups with either high light requirements (e.g., green algae and some cyanobacteria) or tolerance of low-light conditions (e.g., cryptophytes), would be responsive to bottom-up control by light attenuation (H1); the vertical distribution of "brown algae," which is comprised of highly edible or grazer-preferred groups such as chrysophytes and diatoms, would be most susceptible to top-down control by zooplankton (H2); and the vertical distribution of buoyant and motile groups (e.g., cryptophytes and some cyanobacteria) would be sensitive to bottom-up control by thermal stratification, which would allow them to preferentially select a layer for growth and reproduction (H3). Furthermore, we predicted that overall spatial overlap of the spectral groups would be driven primarily by thermal stratification and the consequent formation of vertical resource gradients. This prediction generates two conflicting hypotheses: increased thermal stratification leads to increased spatial overlap by limiting all phytoplankton groups to a narrow region of the water column where resources are optimal (H4A), or increased thermal stratification allows for vertical segregation of spectral groups into distinct layers due to different resource requirements and motility or buoyancy, thereby decreasing spatial overlap (H4B).

Methods

Study sites and field sampling

We sampled the phytoplankton communities and potential top-down and bottom-up drivers in 51 lakes in the Laurentian and Eastern Township regions of southern Québec province, Canada (Fig. 1). Sampling was conducted during the period of maximum summer thermal stratification in July 2004 and July 2005. Both region and sampling year were controlled for in our analysis and shown to have a minimal effect (see below). The lakes were selected to cover gradients of lake size, trophic state, and light availability (Table 1, Fig. 2; Table S1). Importantly, while these lakes span a range of morphometric and chemical characteristics representative of north temperate lakes, they are geographically close enough to experience similar climatic conditions (Fig. S1).

Sampling was conducted at the deepest site in each lake and included a measure of Secchi depth, which was used to calculate photic zone depth (Margalef 1983):

$$Z_{\text{photic}} = 2.79 \times Z_{\text{Secchi}} \quad (1)$$

Integrated samples for phytoplankton were then collected across the photic zone using a flexible polyvinyl chloride tube sampler, and a 125 mL aliquot was preserved using Lugol's solution for later microscope analysis. Integrated tows of zooplankton across the water column (starting at 1 m above the

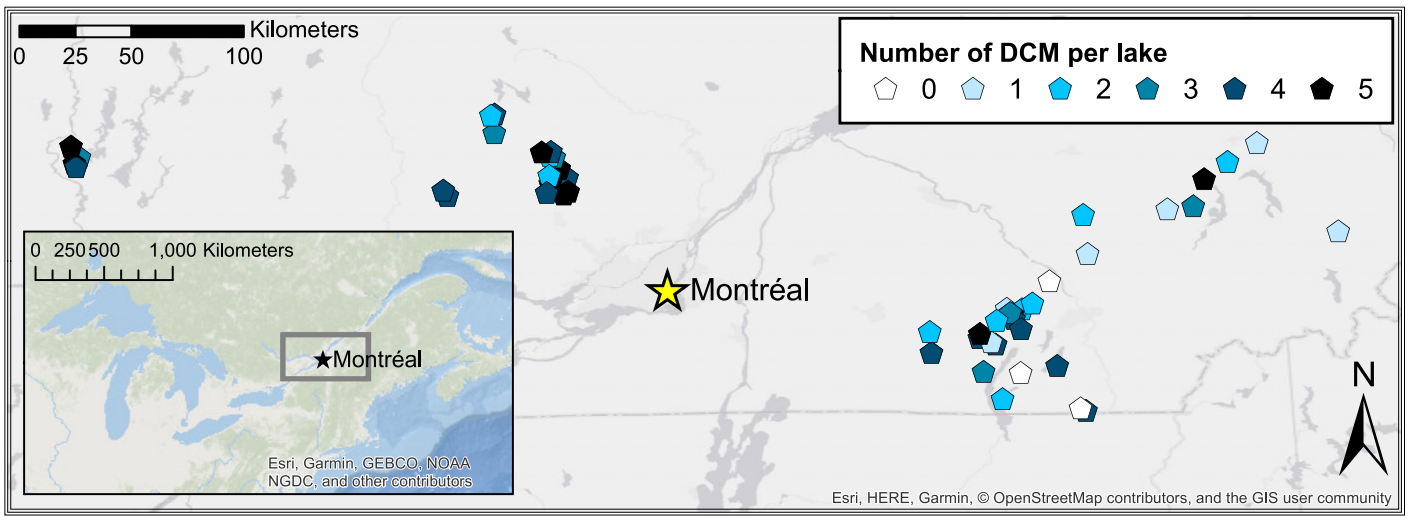

Fig. 1. Map of study lakes in Québec, Canada, with a regional inset map for reference. Each study lake is marked by a hexagon (n = 51). The color of the hexagon indicates the number of DCM present in each lake, with a maximum possible total of five (four spectral group profiles for green algae, cyanobacteria, brown algae, and cryptophytes, and one total biomass profile). Montréal is indicated by the yellow star. The gray rectangle in the inset map indicates our study area.

Table 1. Summary of characteristics of 51 study lakes. Mean phytoplankton biomass was calculated from fluorescence-based profiles across the photic zone.

Lake characteristic	Range	Mean	Median	SD
Maximum depth (m)	1.8–84.8	20.6	16.7	16.8
Volume (m^3)	2.85×10^5–7.29×10^8	3.48×10^7	8.05×10^6	1.06×10^8
Area (km^2)	0.086–18.710	2.392	1.210	3.8
pH	6.56–9.40	7.80	7.70	0.54
Total nitrogen ($\mu g\ L^{-1}$)	166–927	377	333	174
Total phosphorus ($\mu g\ L^{-1}$)	5–102	20	16	15
Dissolved organic carbon ($mg\ L^{-1}$)	2.1–18.5	6.3	5.9	2.7
Absorbance at 440 nm (A_{440})	0.2303–10.3635	1.7433	1.4970	1.6215
Secchi depth (m)	0.75–9.5	3.75	3.5	1.75
Thermocline depth (m)	2.3–16.3	7.4	6.9	3.2
Total zooplankton biomass ($\mu g\ L^{-1}$)	4–362	60	36	76
Mean phytoplankton biomass ($\mu g\ L^{-1}$)	0.4–21.9	3.5	1.9	4.4

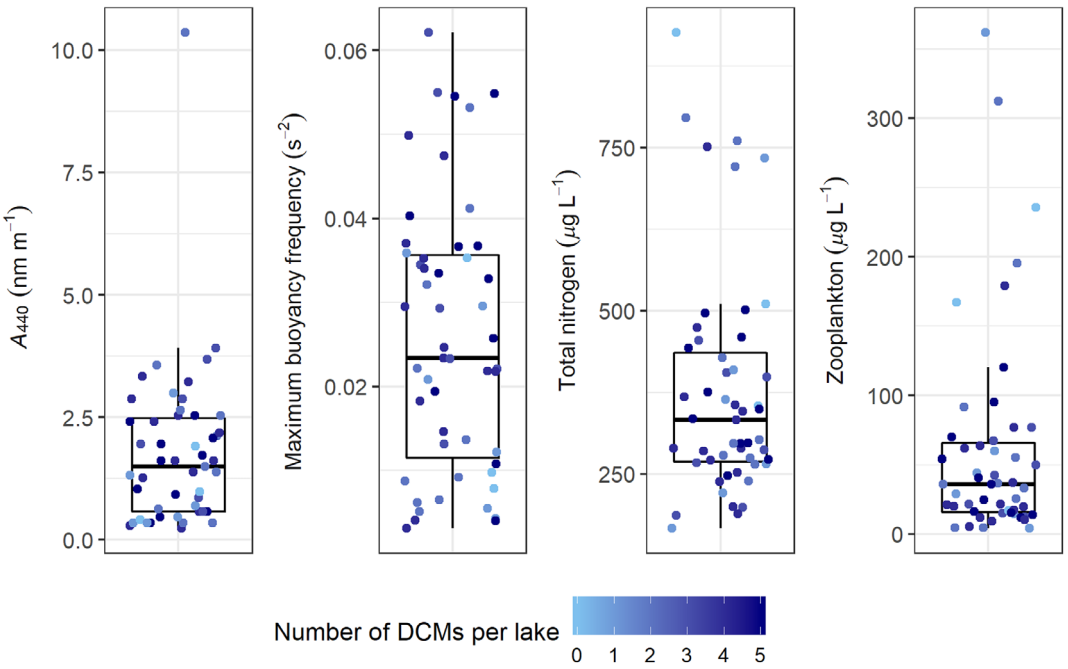

Fig. 2. Range of selected driver variables for regression tree analysis across all 51 study lakes. Driver variables were selected to represent a suite of bottom-up controls (nutrients, light, thermal stratification) as well as top-down control (zooplankton predation) on phytoplankton. Pairwise Spearman's correlation coefficients for all selected driver variables were less than 0.5 (Fig. S3). Number of DCMs per lake is the number of spectral group profiles that exhibited a fluorescence-based biomass peak below the top 10% of the water column (each lake had four spectral group profiles and one total phytoplankton biomass profile, for a maximum possible total of 5 DCMs).

sediment) were collected using a 100 μm mesh net (2 m long with a 0.5 m opening) and fixed in 75% ethanol. In addition, water was collected from a depth of 0.5 m with a 2 L Van Dorn sampler for analysis of total phosphorus (TP), total nitrogen (TN), dissolved organic carbon (DOC), pH, and absorbance at 440 nm as a measure of light attenuation potential. While depth-specific measurements of phytoplankton and zooplankton as well as environmental variables such as nutrients would have been useful, the substantial effort involved in sampling 20–30 lakes within ~1 month each year at the peak of summer stratification precluded depth-specific measurements of all variables.

The vertical distribution of the phytoplankton community was assessed with high-frequency (~10-cm resolution) depth profiles of four phytoplankton spectral groups as well as total phytoplankton biomass. We collected the depth profiles with a FluoroProbe (bbe Moldaenke, Schwentinental, Germany; Catherine et al. 2012) across the top 20 m of the water

column, or the whole water column for lakes < 20 m deep. FluoroProbes are submersible, in situ fluorometers that report biomass of four phytoplankton spectral groups: (1) "green algae" based primarily on Chl *a* and Chl *b* fluorescence, (2) "cyanobacteria" based primarily on phycocyanin fluorescence, (3) "brown algae" based primarily on xanthophyll fucoxanthin and peridinin fluorescence, and (4) "cryptophytes" based primarily on phycoerythrin fluorescence (Beutler et al. 2002). FluoroProbes also report "total biomass," which is the sum of the biomass of the four spectral groups, resulting in five fluorescence-based biomass profiles per lake: one for each spectral group, and one more for total biomass. Hereafter, we will refer to "fluorescence-based profiles" as any of the five profiles collected by the FluoroProbe, and "total biomass" profiles as the subset of FluoroProbe profiles that represents the sum of the four spectral group profiles for each lake.

Our FluoroProbe was calibrated to factory standards using monospecific cultures of the following species to develop algal "fingerprints" for each of the four spectral groups: *Chlorella vulgaris* for green algae, *Microcystis aeruginosa* for cyanobacteria, *Cyclotella meneghiniana* for brown algae, and *Cryptomonas* sp. for cryptophytes (Beutler et al. 2002). FluoroProbes are often used to track the concentration and vertical distribution of these four phytoplankton spectral groups in aquatic ecosystems (Kring et al. 2014). In addition, FluoroProbes simultaneously record water temperature at the same resolution as fluorescence.

Laboratory analyses

All water chemistry samples were analyzed following standard methods. TP and TN were determined after alkaline persulfate digestion using an Ultraspec 2100 pro spectrophotometer (Biochrom, Cambridge, U.K.) and an Alpkem autoanalyzer (OI Analytical, College Station, TX, U.S.A.), respectively. DOC of filtered water samples (surfactant-free membrane filters) was determined after acidification with 5% sulfuric acid and sodium persulfate oxidation on a 1010 TOC analyzer (OI Analytical, College Station, TX, U.S.A.). The absorption coefficient at 440 nm (A_{440}) of filtered (Whatman GF/F) water samples was measured using a 2 cm quartz cuvette and calculated as in (Kirk 2011), where 2.303 is the factor for converting natural to decadal logarithms:

$$A_{440} = 2.303 \times \left(\frac{\text{absorbance at 440 nm}}{0.02\,\text{m}} \right) \quad (2)$$

To characterize the taxa represented within each spectral group, phytoplankton in fixed whole-water samples were identified to species and counted using the Ütermohl method at 640× on an Olympus (model IX 71) inverted microscope. Subsamples were counted until no new species were seen in five consecutive fields of view, and the counting chamber was scanned along one transect at 200× for rare species. Biovolumes of each species were estimated based on measurements of major dimensions of ~20 cells of each taxon and calculated according to corresponding geometric forms (Hillebrand et al. 1999). We subsequently aggregated biovolumes of species to genus and used genus-level data for all our analyses.

Zooplankton were identified on Olympus dissecting (20–32×) and upright (200–400×) microscopes to the species level. Individuals were counted in 2 mL concentrated subsamples until 200 organisms had been enumerated, and subsamples were taken until no new species were found after two consecutive subsamples. Zooplankton biomass was estimated by measuring the length of the first 10 individuals of each species, which was then converted to biomass using previously published length-weight regressions (McCauley 1984). We subsequently aggregated biomass of all species to total biomass for each lake and used total zooplankton biomass for all of our analyses. However, we note that both copepods and cladocerans were commonly present across the study lakes, with 33 lakes dominated by cladoceran taxa and 18 by copepods (Table S1).

Verification of FluoroProbe data and spectral group taxa

Because FluoroProbe determination of spectral group biomass is based on the fluorescence of a set of pigments that are found in multiple phytoplankton taxa with varying pigment concentration-to-biomass ratios, it is important to validate fluorescence-based data with other measures of the phytoplankton community (Fennel and Boss 2003; Derks et al. 2015; Selmeczy et al. 2016). While our sampling campaign did not permit multiple depth samples of phytoplankton at each lake, we were able to collect integrated tows across the photic zone of each lake and use these samples to verify the dominant phytoplankton taxa within each FluoroProbe spectral group across lakes (Text S1). This verification was done a priori as a check on the FluoroProbe data.

We found that mean biomass across the photic zone reported by the FluoroProbe corresponded well to biovolume calculated from microscope counts for most spectral groups across our study lakes (Figs. S2, S3). Genera identified microscopically were assigned to spectral groups based on the following taxonomic associations: chlorophytes, euglenoids, and desmids were classified as the green algae spectral group; dinoflagellates, diatoms, and chrysophytes were classified as the brown algae spectral group; cyanobacteria were classified as the cyanobacteria spectral group; and cryptophytes were classified as the cryptophyte spectral group.

After running our regression tree analysis based on FluoroProbe data, we also compiled lists of the top 10 dominant genera in each spectral group across the study lakes to aid in interpretation of FluoroProbe analysis results. We used the top 10 dominant genera because this included all genera that were the dominant genus within each spectral group in two or more lakes. Dominance within each lake was determined according to biovolume estimates from microscope counts. Across lakes, dominance was determined by tallying of

the number of lakes in which a genus was the dominant representative of its spectral group.

Calculation of thermal stratification metrics

To assess thermal stratification in our study lakes, we used temperature profiles obtained from the FluoroProbe (accuracy ± 0.1°C) to calculate seasonal thermocline depth and the maximum buoyancy frequency, or Brunt-Väisälä frequency, in the top 20 m of the water column following methods outlined in Read et al. (2011). Fifty of 51 lakes had an identifiable seasonal thermocline. We performed calculations using rLakeAnalyzer (Albers et al. 2018), an open-source package to calculate thermal stability metrics in lakes in the R statistical environment (R version 3.5.2, R Core Development Team, 2018). We chose these two metrics because they are localized metrics that enabled characterization of thermal stability in the region of the water column where phytoplankton are most likely to occur (Read et al. 2011) and for which we had corresponding phytoplankton spectral group data. Furthermore, these metrics do not require a bathymetric or temperature profile of the whole water column, which were not available for some lakes.

Calculation of depth profile characteristics

To characterize phytoplankton vertical distributions across our study lakes, we analyzed FluoroProbe depth profiles. While the use of fluorescence-based biomass data comes with some caveats, such as the possibility of non-photochemical quenching under high light conditions (Derks et al. 2015), increased cell pigment concentration at depth (Fennel and Boss 2003), and misclassification of fluorescence signals to spectral groups due to mixed assemblages (Selmeczy et al. 2016), we argue that there is currently no better methodological alternative for studies explicitly examining high-frequency vertical distributions of phytoplankton across many lakes. In cross-site studies it is critical to use comparable methods across study lakes, which requires an easily portable instrument such as the FluoroProbe. As a check on the FluoroProbe, we collected depth-integrated phytoplankton samples for microscopic analysis from all 51 lakes (described above) to inform our interpretation of all fluorescence-based data.

We used fluorescence profiles to calculate four different metrics describing phytoplankton vertical distributions for each spectral group measured as well as total biomass: mean biomass aggregated across the photic zone, depth of maximum fluorescence-based biomass, width of the fluorescence-based biomass peak (if present), and spatial overlap of spectral group profiles (Fig. 3). Taken together, these metrics describe the magnitude, depth, breadth, and co-occurrence, respectively, of the spectral groups in each depth profile.

Two of our four vertical distribution metrics (depth of maximum fluorescence-based biomass and peak width) were depth-specific, and this presented a challenge as our study includes lakes ranging in depth from 1.8 to 84.8 m (Table S1). Phytoplankton occurring in a fluorescence-based biomass peak with a width of 1 m and at a depth of 1 m in a very shallow lake are likely not experiencing or responding to the same

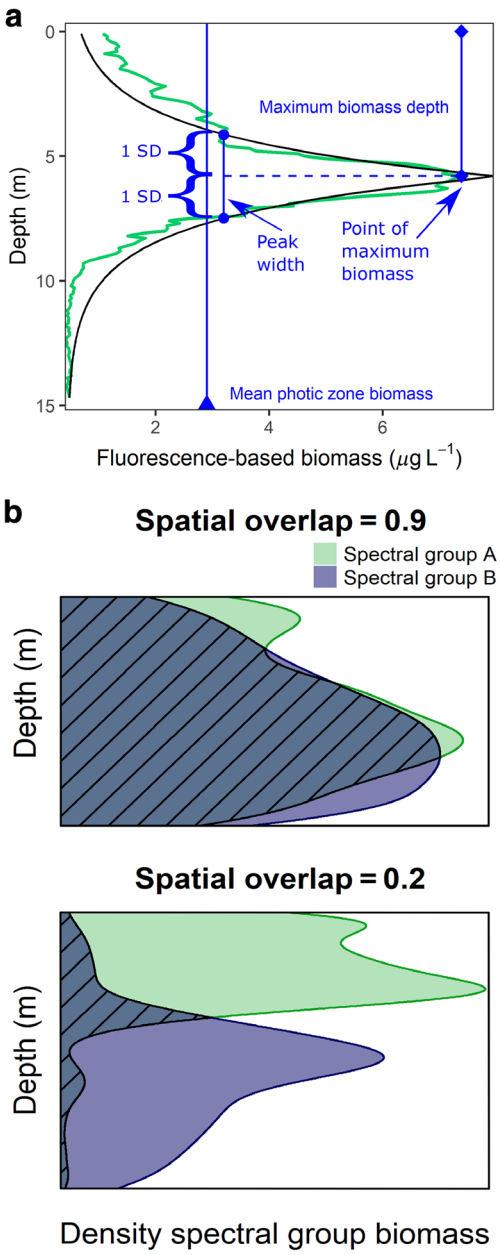

Fig. 3. Phytoplankton vertical distribution characteristics. (**a**) Example depth profile depicting three of the four vertical distribution characteristics: Mean biomass across the photic zone, the depth of maximum biomass standardized to lake depth, and peak width, calculated by running a curve-fitting procedure on each depth profile and then calculating the width of the fitted curve at ± 1 SD from the peak of the curve, which corresponds to the maximum biomass value observed in the profile. Peak width was standardized to lake depth. (**b**) Example depth profiles depicting spatial overlap, or the proportion of depth profiles of two different spectral groups that overlap.

environmental conditions as in a peak of the same width and depth in a very deep lake; thus, we considered it necessary to standardize these two metrics across lakes. To avoid standardizing the vertical distribution metrics using a variable that was to be subsequently used as a driver in our analysis (i.e., thermal stability or light attenuation), we standardized by dividing the depth of maximum biomass or the width of the peak by the maximum depth of each lake to permit comparisons among lakes. We recognize that in some cases, this standardization may complicate interpretation of results relating to these two vertical distribution metrics, which we address in the Discussion.

We classified a fluorescence-based vertical profile as exhibiting a DCM if: (1) a peak was present, with a biomass maximum at least 0.5 μg L^{-1} greater and 1.5× the magnitude of mean photic zone biomass (following Leach et al. 2018); and (2) the peak was deep, with a depth of maximum biomass below the top 10% of the water column. Not all fluorescence peaks met the second criterion to be classified as a DCM, but regardless, we estimated depth of maximum biomass and peak width for every fluorescence peak. The width of all fluorescence peaks was calculated by running a curve-fitting procedure on each depth profile following Leach et al. (2018) and then finding the width of the fitted curve at plus and minus 1 SD from the peak of the fitted curve, which is equivalent to the maximum biomass value observed in the profile (Fig. 3a; Script S1; Script S2; all R scripts accessible at https://github.com/melofton/Top-down-vs.-bottom-up-control-of-DCMs). All profiles were manually inspected to ensure goodness-of-fit of the curve-fitting procedure.

Spatial overlap, or the proportion of spectral group depth profiles that overlap, was calculated following methods in Beisner and Longhi (2013) (Fig. 3b; Script S3). Briefly, a kernel density function was fit to each standardized spectral group profile, and the mean proportion of overlap between all pairwise combinations of spectral group vertical distributions within a lake represents spatial overlap, a unitless index ranging from 0 (no overlap among spectral groups vertical distributions) to 1 (complete overlap among all spectral groups; Beisner and Longhi 2013). If a spectral group or total biomass profile did not have a defined peak, we only calculated mean photic zone biomass and spatial overlap for that profile.

Regression tree analysis

We used a regression tree analysis to assess the relative importance of top-down and bottom-up controls on each of the four depth profile characteristics. Regression trees identify the most important predictors of a continuous response variable by dividing the variable into sequentially more homogeneous groups based on the values of the predictors (Breiman et al. 1984). They are well-suited for use with ecological data because they can use both categorical and continuous explanatory variables as input (although by definition a regression tree has a continuous response variable), identify relationships between drivers and responses even when those relationships are non-linear, and provide clear, readily interpretable output (De'ath and Fabricius 2000).

When conducting regression tree analyses, it is important to ensure that driver variables are not strongly correlated, as this may compromise the ability to identify the most important driver of the response variable. To ensure that the driver variables for our regression tree analysis were not too collinear, we conducted Spearman's correlations among all candidate driver variables and selected the driver variables representing both bottom-up and top-down control for which Spearman's ρ coefficients were <0.5 (Fig. S5): total zooplankton biomass in the photic zone (top-down), A_{440} as a measure of water color and therefore light attenuation potential (bottom-up), maximum buoyancy frequency in the top 20 m of the water column as a metric of thermal stratification (bottom-up), and total nitrogen (TN) to represent lake trophic state (bottom-up). We used TN to represent nutrient conditions because the first axis of a principal components analysis incorporating both TN and TP (following Hamre et al. 2017) showed that most of the variation among study lakes was due to TN (Fig. S4), and TN and TP concentrations were too highly correlated (ρ = 0.80) to include as separate drivers in the regression tree analysis. Collinearity among response variables is not a concern because separate regression tree analyses are conducted for each response variable. Before running the regression tree analysis, all driver and response variable distributions were tested for Pearson's moment coefficient of skewness with and without a natural log transformation. On the basis of that test, A_{440}, total photic zone zooplankton biomass, mean photic zone phytoplankton biomass, and standardized depth of maximum biomass were natural log-transformed to reduce skewness prior to analysis.

Using the selected driver variables, we constructed regression trees to predict mean photic zone biomass, standardized depth of maximum biomass, and peak width for total phytoplankton biomass and each of the four spectral groups individually from the 51-lake dataset. We also constructed a single additional tree to predict the mean spatial overlap between all pairwise combinations of spectral groups in a lake (n = 16 trees total; Figs. S6–S10). All trees were constructed using the *rpart* package in the R statistical environment (Therneau and Atkinson 2019). We set the maximum depth of each tree to one split to focus on the strongest driver of each DCM characteristic.

Validation of regression tree analysis

To validate and test the robustness of our regression tree analysis, we conducted a cross-validation procedure with 1000 repetitions and rejected trees if the cross-validation error ± 1 SE of the tree was not within the range of the minimum cross-validation error ± 1 SE (Fig. S11; Breiman et al. 1984; Harper et al. 2011). To further test the robustness of our regression tree results we ran the regression tree analysis

sequentially withholding one lake at a time to verify that a single lake was not driving our regression tree results (Table S2). All 16 trees from our regression tree analysis were replicated >75% of the time in the hold-one-out analysis, both in terms of the primary driver identified and the breakpoint value of that driver at the first split. Seven trees were replicated 100% of the time in the hold-one-out analysis and another five trees were replicated ≥90% of the time (Table S2).

We also checked whether our regression tree analysis was sensitive to landscape distribution of our study lakes or the year in which the study lakes were sampled. To test for regional effects, we ran the analyses using region (either Laurentian or Eastern Townships) as a categorical predictor variable; only one tree (standardized depth of maximum biomass for total biomass) included region as an important driver. When running the analyses using sampling year (either 2004 or 2005) as a categorical predictor variable, no trees returned sampling year as the primary driver of any vertical distribution characteristic.

Results

Prevalence of DCM across lakes and spectral groups

Biomass peaks were prevalent in the study lakes across all fluorescence profiles, and the majority of fluorescence peaks were classified as DCMs. Of the 255 fluorescence-based depth profiles (encompassing both the four spectral group profiles and total biomass profiles that summed the four spectral groups) from the 51 lakes, 72% displayed peaks, including 55% of green algae profiles, 59% of cyanobacteria profiles, 90% of brown algae profiles, 76% of cryptophyte profiles, and 78% of total biomass profiles. Furthermore, 48 of 51 lakes displayed a DCM in at least one of the five FluoroProbe depth profiles collected at that lake, with 24% of lakes displaying DCMs in all depth profiles and another 32% displaying DCMs in four of five depth profiles (Figs. 1, 2). Overall, 86% of all fluorescence peaks were classified as DCMs, with the prevalence of DCMs among spectral groups ranging from 68% of peaks in the green algae to 92% among cryptophytes. In total biomass profiles, 73% of all peaks were classified as DCMs.

Spectral groups differ in depth and peak width

The spectral groups exhibited significantly different biomass maximum depths (Kruskal-Wallis $\chi^2 = 15.5$, $p = 0.001$; Fig. 4b,c). Green algae generally exhibited the shallowest biomass maximum depths, usually occurring in the top 25% of the water column (mean standardized maximum biomass depth = 0.22 ± 0.24, 1 SD), while cyanobacteria and cryptophytes were often the deepest-occurring spectral groups (mean standardized maximum biomass depths = 0.41 ± 0.29 and 0.39 ± 0.29, respectively). However, both cyanobacteria and cryptophytes exhibited bimodal standardized biomass maximum depth distributions, often exhibiting peaks both at relatively shallow depths in deep lakes ($Z_{max} \geq 10$ m) and relatively deep depths in shallow lakes (Fig. 4b,c). In shallow

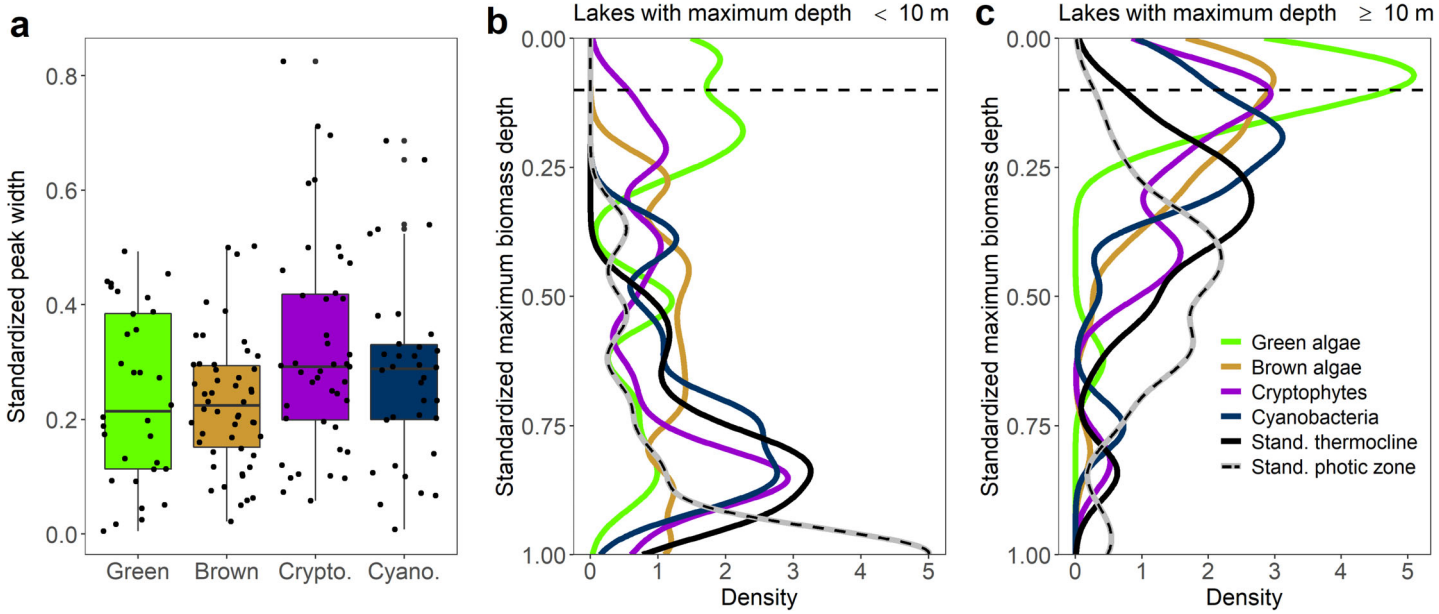

Fig. 4. (**a**) Bar plot of peak width for each spectral group. Peak width was standardized to the maximum depth of each lake. (**b**) Kernel density plot of standardized maximum biomass depth of all spectral groups, standardized thermocline depth, and standardized photic zone depth for all study lakes with a maximum depth less than or equal to 10 m. Note that many shallow lakes had photic zones (calculated from Secchi depth) that extended to the bottom of the lake. (**c**) Kernel density plot of standardized maximum biomass depth of all spectral groups, standardized thermocline depth, and standardized photic zone depth for all study lakes with a maximum depth greater than 10 m. The horizontal dotted line in panels (**b**) and (**c**) represents the depth below which peaks were defined as DCM for our study (below the top 10% of the water column).

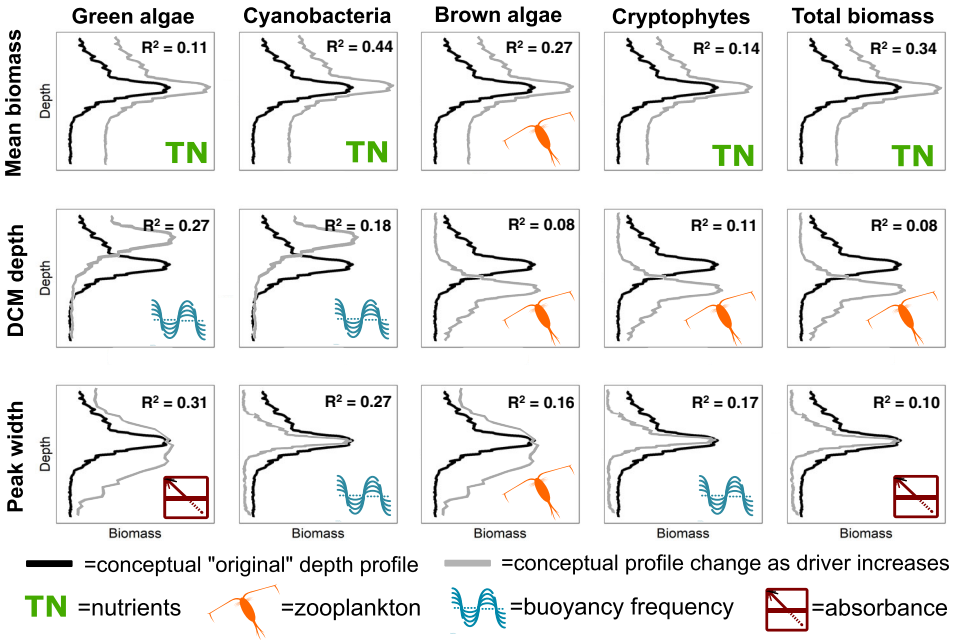

Fig. 5. Conceptual figure illustrating results of the regression tree analysis. Symbols in the bottom right corner of each plot represent the primary driver for each vertical profile characteristic as identified in the regression tree analysis. The R^2 value at the top of each plot is the proportion of variance explained by the primary driver, or first split. Black lines represent a conceptual "original" or baseline depth profile, while gray lines provide a conceptual representation of how that depth profile would change as the primary driver increases. Note that all depth profiles in this figure are stylized representations of regression tree results and do not represent actual FluoroProbe data.

lakes, these two spectral groups usually occurred at the depth of the thermocline, while in deep lakes, they often occurred above it. Peaks of brown algae usually occurred mid-profile between green algae and cyanobacteria/cryptophytes, with a mean standardized maximum biomass depth of 0.32 ± 0.27, corresponding closely with the mean standardized maximum biomass depth for total biomass (0.34 ± 0.26). In all, 191 of 255 depth profiles (75%) had biomass maximum depths above the thermocline in the mixed layer of the epilimnion (Fig. 4b, c). In addition, 91% of all biomass maximum depths were above the photic zone (defined as $2.79 \times Z_{\text{Secchi}}$), and this was especially prevalent in shallow lakes. Occasionally, we observed a cryptophyte or cyanobacterial peak at or below the depth of the photic zone in deep lakes (Fig. 4b,c).

Spectral groups also displayed marginally significant differences in the width of their peaks (Kruskal-Wallis $\chi^2 = 7.1$, $p = 0.07$, Fig. 4a). Brown algae consistently exhibited narrow standardized peak widths (0.23 ± 0.11), while cryptophytes had the broadest but also the most variable peak widths (0.32 ± 0.18). The mean standardized peak width for green algae was similarly narrow but more variable than for the brown algae (0.24 ± 0.15), while cyanobacteria exhibited peaks of both intermediate breadth and variability (0.28 ± 0.16). As they represent the sum of different spectral group peaks, total fluorescence peaks were generally wider and more variable than peaks for individual spectral groups (mean 0.35 ± 0.22).

Top-down and bottom-up control of total biomass

Both top-down and bottom-up variables were important drivers for different characteristics of total biomass vertical distributions. Mean total photic zone biomass was positively associated with higher nutrients (i.e., higher TN; Fig. S6), while peak width was inversely associated with A_{440}, so as light attenuation increased, peak width tended to narrow (Fig. 5; Fig. S6). Standardized maximum biomass depth was positively associated with higher total zooplankton biomass in the photic zone, indicating that when zooplankton were abundant, standardized maximum biomass depths tended to be deeper. In sum, bottom-up drivers were most important for two of three total biomass depth profile characteristics, but no single driver emerged as a dominant control over the vertical distribution of total biomass depth profiles.

Bottom-up drivers control green algae and cyanobacteria

Vertical distributions of both green algae and cyanobacteria were exclusively driven by bottom-up controls, although the most important bottom-up driver varied for different characteristics of the depth profile, especially for green algae (Fig. 5; Figs. S7, S8). Mean photic zone biomass for both green algae and cyanobacteria was positively associated with higher nutrients, similar to the total phytoplankton profiles. For cyanobacteria biomass, both standardized maximum biomass depth and peak width were controlled by maximum buoyancy frequency: as stratification increased, cyanobacterial peaks

tended to become both shallower and narrower. Higher maximum buoyancy frequency was also associated with shallower standardized maximum biomass depths for green algae biomass, but green algae peak width was driven by light attenuation: as light attenuation increased, green algae peak widths tended to become broader. This result was the opposite of the regression tree result for peak width of total phytoplankton biomass, in which high light attenuation was associated with narrow peak widths. Overall, cyanobacteria were the most sensitive spectral group to thermal stratification, which emerged as the primary driver of two of three cyanobacterial depth profile characteristics. While green algae were similarly sensitive to bottom-up controls as cyanobacteria, no single driver emerged as the dominant control of green algae vertical distributions.

Zooplankton important to brown algae distribution

Unlike other spectral groups, total zooplankton biomass in the photic zone emerged as the single strongest driver for all brown algae vertical distribution characteristics (Fig. 5; Fig. S9). Higher zooplankton biomass was associated with both deeper maximum biomass depths and broader peak widths of brown algae. While mean photic zone biomass of other spectral groups was positively associated with higher nutrients, mean photic zone biomass of brown algae was positively associated with higher zooplankton biomass. Of all the groups, brown algae were both the most sensitive to zooplankton and their depth profile characteristics were most consistently sensitive to a single environmental variable.

Top-down and bottom-up drivers of cryptophytes

Cryptophytes were the only spectral group to exhibit both top-down and bottom-up controls on their vertical distribution, and in that respect most closely mirrored the total phytoplankton biomass results (Fig. 5; Fig. S10). Similar to total biomass, mean photic zone biomass of cryptophytes was positively associated with higher nutrients, while higher zooplankton biomass was associated with deeper cryptophyte maximum biomass depths. However, unlike the total biomass profiles, narrower peak widths for cryptophytes were associated with strongly stratified water columns, not high light attenuation. While green algae and cyanobacteria biomass distributions were consistently sensitive to bottom-up drivers and brown algae biomass distribution characteristics were always strongly associated with zooplankton biomass, cryptophyte biomass vertical

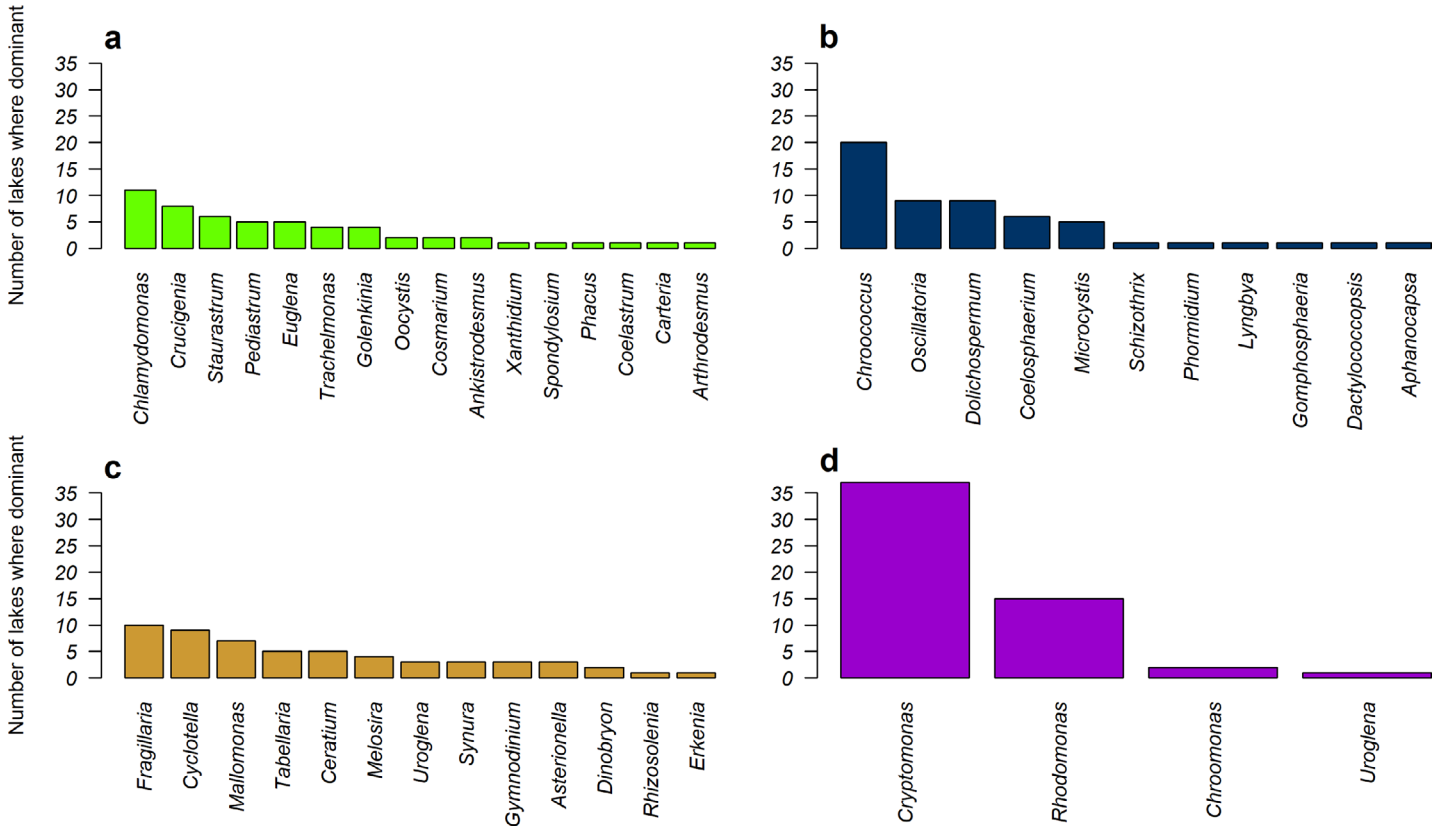

Fig. 6. Frequency distribution of the dominant genera in each phytoplankton spectral group across lakes: (**a**) green algae, (**b**) cyanobacteria, (**c**) brown algae, and (**d**) cryptophytes. Dominance was determined by biomass concentration from microscope counts (micrograms per liter). Genera that were not dominant in any lake are not shown.

distributions were sensitive to both bottom-up and top-down controls.

Spatial overlap

Co-occurrence in the water column among spectral groups as designated by high spatial overlap scores was inversely associated with maximum buoyancy frequency in the top 20 m (R^2 = 0.26), indicating that strongly stratified water columns had less spatial overlap among spectral groups (Fig. S6).

Taxa comprising each spectral group across lakes

When we microscopically identified the phytoplankton genera that were the dominant representatives of each spectral group in each of our study lakes, we found that spectral groups within a lake were likely comprised of multiple taxa exhibiting a variety of life history strategies and functional traits across the 51 lakes.

While green algae were the least dominant spectral group in the study lakes in biomass according to both the FluoroProbe and microscope counts, they were also the most diverse spectral group: across the 51 lakes, there were 16 different green algae genera that were identified as the dominant representative within that spectral group in at least one lake. There were five green algae genera that were the dominant representative of the green algae spectral group in five or more lakes: *Chlamydomonas, Crucigenia, Staurastrum, Pediastrum*, and *Euglena* (Fig. 6). In addition, mean photic zone green algae biomass reported by the FluoroProbe was best correlated with chlorophyte abundance in microscope counts (Spearman's r = 0.36; Fig. S3), further indicating that the green algae spectral group was mostly comprised of taxa in the chlorophyte group.

Brown algae, which were identified as the most dominant spectral group across the study lakes by both the FluoroProbe and the microscope counts, was the next most diverse spectral group (13 different genera identified as the dominant brown algae representative in at least one study lake). Among these genera, *Fragilaria, Cyclotella, Mallomonas, Tabellaria*, and *Ceratium* were identified as the dominant brown alga in five or more lakes (Fig. 6). Interestingly, although the five most dominant genera include diatoms, chrysophytes, and dinoflagellates, mean photic zone brown algae biomass reported by the FluoroProbe was best correlated with chrysophyte abundance (Spearman's r = 0.51; Fig. S3), suggesting that brown algae reported by the FluoroProbe was mostly comprised of chrysophytes.

The cyanobacteria spectral group had 11 genera identified as the dominant cyanobacteria representative in at least one lake (Fig. 6), with *Chroococcus* being the dominant cyanobacterial genus in 20 lakes and *Oscillatoria, Dolichospermum, Coelosphaerium*, and *Microcystis* being the dominant cyanobacterial genus in 5–10 lakes each (Fig. 6). There were only four genera in the cryptophyte spectral group that were the dominant representative of that group in at least one study lake but Cryptophyta is also a smaller, less diverse taxonomic category than the other spectral groups. The two most common cryptophyte genera were *Cryptomonas* (dominant cryptophyte in 37 lakes) and *Rhodomonas* (dominant cryptophyte in 15 lakes).

Discussion

Our study across 51 north temperate lakes demonstrates that both top-down and bottom-up drivers affect the vertical distribution of phytoplankton and characteristics of DCMs, and that their relative importance varies across different phytoplankton spectral groups. This work integrates ecological questions about the relative importance of top-down vs. bottom-up controls with limnological research on the drivers of DCM characteristics in aquatic ecosystems.

We found that bottom-up control via nutrients was the most important driver of mean photic zone biomass across several phytoplankton spectral groups, supporting the idea that top-down control weakens at the zooplankton-phytoplankton trophic link and phytoplankton abundance is primarily driven by bottom-up controls (McQueen et al. 1989; Jeppesen et al. 2003; Du et al. 2015; Yuan and Pollard 2018). However, our findings also suggest that zooplankton can exert an important top-down effect on phytoplankton vertical distribution and that bottom-up control of phytoplankton vertical distribution can occur via multiple mechanisms (including light and thermal stratification), not just nutrients. Below, we consider how the functional traits of dominant genera within each spectral group may inform potential mechanisms behind top-down and bottom-up controls of phytoplankton vertical distribution and DCM characteristics.

Light attenuation important for total biomass

Our hypothesis H1 that vertical distributions of taxa with either high light needs (e.g., green algae, cyanobacteria that form surface blooms) or low-light tolerance (e.g., cryptophytes, metalimnetic cyanobacteria) would be sensitive to water color as a proxy for light attenuation was only partially supported by the regression tree analysis. However, light attenuation was important when considering vertical distribution of total phytoplankton biomass: lakes with high light attenuation potential exhibited narrower total biomass peaks, suggesting that high light attenuation narrows the zone in the water column where the phytoplankton assemblage can thrive. Our results support previous work that found light to be an important driver of total Chl *a* and total phytoplankton biomass DCMs in a range of lakes (Varela et al. 1994; Hamilton et al. 2010; Leach et al. 2018). It is possible that this result is driven by the dominance of light-sensitive taxa in the cryptophyte and green algae spectral groups in our study lakes, such as *Cryptomonas, Chroococcus*, and *Chlamydomonas* (Fig. 6; Clegg et al. 2004; Yang et al. 2015; deNoyelles et al. 2016). However, as we do not have depth profiles of microscopically identified taxa, we cannot definitively state

which taxa are driving the sensitivity of peak width to light attenuation.

Among individual spectral groups, only green algae were affected by light as a primary driver, supporting H1, but the result was non-intuitive: rather than being limited to shallow depths or narrow zones of the water column in lakes with high light attenuation, higher light attenuation potential was associated with broader peaks in the green algae (Fig. 5). This might represent a diverging functional response among dominant genera within the green algae spectral group (Fig. 6). *Chlamydomonas* and *Euglena*, two dominant genera observed in the study lakes that are capable of mixotrophy, might remain in the metalimnion in high light attenuation environments and increase their energy production via DOC uptake or phagotrophy while non-mixotrophic taxa congregate close to the surface, resulting in an overall broader peak of the green algae spectral group when light attenuation is high (Cramer and Myers 1952; Clegg et al. 2004; Tittel et al. 2005). Another possibility is that this result was affected by our chosen method for depth standardization for biomass maxima (see *Caveats of depth standardization* below). In sum, we found light to be a more important predictor of vertical distribution of total phytoplankton than of any individual spectral group.

Nutritious taxa are sensitive to top-down control

We found that brown algae and cryptophytes were most sensitive to zooplankton as a driver of their vertical distribution, in support of our hypothesis H2 that highly edible taxa would be most sensitive to potential top-down control by zooplankton grazing (Holm et al. 1983; Brett et al. 2000, 2006; Hansson et al. 2019). The brown algae spectral group, likely comprised of predominantly chrysophytes in our study lakes (Fig. S3), exhibited broader peaks in the presence of high zooplankton biomass, and both brown algae and cryptophytes had deeper maximum biomass depths when zooplankton biomass was high (Fig. 5). This may be due to zooplankton preferentially grazing at depths of high brown algae biomass, leading to broader, more diffuse peaks (Christensen et al. 1995), as well as zooplankton preferentially grazing down brown algae and cryptophyte biomass in the epilimnion, leading to deeper maximum biomass depths (Pilati and Wurtsbaugh 2003; Brett et al. 2006).

Although the relative abundance of inedible cyanobacteria has previously been shown to be indirectly increased by preferential grazing of zooplankton on other taxa (Lynch and Shapiro 1981; Holm et al. 1983), in our case, we found that cyanobacterial biomass was most responsive to bottom-up control by nutrients, and that the effect of zooplankton was most pronounced on the vertical distributions of more palatable brown algae.

We interpret the positive association between zooplankton biomass and mean photic zone biomass of brown algae as bottom-up control of zooplankton by brown algae rather than top-down control of brown algae by zooplankton. Positive correlations in predator–prey abundance generally signify bottom-up control (Bunnell et al. 2014). As both cryptophyte and brown algae maximum biomass depths were driven by zooplankton and together these two groups represent the dominant spectral groups in 38 of 51 study lakes, these two prey groups are likely driving the result that maximum biomass depths of total biomass profiles were also deeper when zooplankton were abundant.

Strong stratification leads to shallow, narrow peaks

Our hypothesis H3 that vertical distributions of motile or buoyant taxa would be the most sensitive to thermal stratification was supported by our data. We predicted that stable thermal conditions would allow motile and buoyant taxa to select an optimal depth for growth and reproduction based on resource gradients (H3). Three of the five dominant genera of cyanobacteria in our study lakes (*Coelosphaerium, Dolichospermum*, and *Microcystis*) are known to produce gas vesicles or use carbohydrate ballast to regulate buoyancy (Oliver 1994; Visser et al. 1997; Medrano et al. 2016), and cyanobacteria were the most sensitive spectral group to thermal stratification. In addition, the peak width of the highly motile cryptophytes was also driven by stratification. Both of these findings support our hypothesis. However, as it is difficult to tease apart the effects of thermal stratification from lake depth in our dataset, continued investigation into the effects of thermal stratification on the vertical distribution of phytoplankton with different functional traits is warranted.

Spatial overlap driven by stratification

Spatial overlap, or the degree of overlap in the distributions of phytoplankton spectral groups, decreased as thermal stratification increased, supporting earlier analyses by Beisner and Longhi (2013). Thus, as conditions became favorable for phytoplankton spectral groups to optimize their depth for growth and reproduction via the development of a stable water column, spectral groups exhibited distinct vertical segregation. This finding supports our hypothesis H4B that increased thermal stratification would decrease spatial overlap. As such, our results support previous work suggesting that in vertically heterogeneous (stratified) systems, competitive outcomes between the same two taxa may be different in different regions of the water column and are predicated on both resource gradients and taxon life history strategy (Yoshiyama et al. 2009; Ryabov and Blasius 2014). Our alternative hypothesis H4A that increased thermal stratification would promote aggregation of phytoplankton groups into the narrow zone in the water column where conditions are suitable for growth (thereby increasing spatial overlap) was not supported by our synoptic study, but could perhaps occur in other conditions, such as within a single lake over time.

Caveats of depth standardization

We chose to standardize two of our vertical distribution metrics (maximum biomass depth and peak width) to maximum lake depth to permit comparison across lakes with a wide range of depths. However, this standardization can present some challenges in interpreting the regression tree results for these two metrics, which we examine below.

We found that strong thermal stratification caused green algae, cryptophyte, and cyanobacteria spectral group peaks to become either shallower, narrower, or both (Fig. 5). Green algae peaks became shallower in water columns with high maximum buoyancy frequency, while cryptophyte peaks became narrower, and cyanobacterial peaks became both shallower and narrower. The formation of narrow, steep-sloped peaks, known as thin layers, under strong thermally stratified conditions due to enhanced steepness of nutriclines and other chemical gradients has been documented in other studies (Durham and Stocker 2011). However, there is less precedent for the finding that thermal stratification leads to shallower biomass peaks, as we observed for green algae and cyanobacteria. In our case, this is likely because our study lakes are composed of both shallow, warm lakes with low thermal stratification where phytoplankton can persist relatively deep into the water column via mixing, and deep lakes with highly stable thermal stratification where phytoplankton with high light requirements or tolerance are restricted to a relatively (to lake depth) thin layer at the top of the water column. Thus, when we standardized maximum biomass depth to the maximum depth of the lake, we see that the shallow, mixed lakes had relatively deep maximum biomass depths and deep, stratified lakes had relatively shallow maximum biomass depths (Fig. 4b,c).

Additionally, we found that high light attenuation leads to broader peaks of green algae, a non-intuitive result. We believe this response might be representative of divergent life history strategies among different taxa comprising the green algae spectral group, with some taxa moving to the metalimnion to pursue a mixotrophic strategy while others move closer to the lake surface in response to decreased light availability. However, it is also possible that peaks simply tend to be wider in shallow lakes relative to the depth of the water column. Furthermore, many of the shallow lakes in our dataset do exhibit high light attenuation (Fig. S12). So if shallow lakes are associated with broad peak width, it could lead to our result of high light attenuation also being associated with broad peak width. However, if this were the case, we would expect to see this result across all spectral groups and not just the green algae. Because high light attenuation is associated with broad peak width only in the green algae, the more likely explanation is that taxa within this spectral group are exhibiting divergent responses to high light attenuation, resulting in an overall broader peak width.

Considerations for future work

Future research considering the balance of top-down vs. bottom-up control on phytoplankton vertical distributions as mediated by functional traits would benefit from measurement of resource gradients and zooplankton grazing rates, depth-specific microscope identification of phytoplankton and zooplankton taxa, measurement of phytoplankton functional traits, improved physical data to examine phytoplankton entrainment and mixing effects, and consideration of how top-down and bottom-up control vary in a single lake over time. Because we did not have depth profiles of nutrients in our study lakes, we could only infer how nutriclines might be changing under stratified conditions. However, we note that 75% of all depth profiles in our study lakes exhibited biomass maximum depths above the thermocline; as such, we believe that nutrient conditions at 0.5 m depth are representative of conditions experienced by the majority of phytoplankton peaks occurring in the mixed layer. In addition, as we did not have measurements of zooplankton grazing rates, we assumed that zooplankton grazing increased as zooplankton biomass increased (Lampert et al. 1986).

Previous researchers have emphasized the importance of using microscopic count data as a complement to fluorescence depth profiles as changes in fluorescence may be due to increases in cellular pigment concentration rather than changes in biomass (Fennel and Boss 2003; Derks et al. 2015; Selmeczy et al. 2016). While we had depth-integrated cell count data that allowed us to determine which phytoplankton taxa were most likely represented by the spectral groups in our study lakes, we would have benefitted from depth-specific data to identify the taxon or taxa responsible for each of the fluorescence peaks. This would have been particularly useful for the cryptophyte spectral group, for which biovolumes calculated from microscope counts were less well-correlated with FluoroProbe biomass in our study lakes than other spectral groups (Fig. S2). Further, site-specific in situ measurement of functional traits of phytoplankton (such as presence or absence of gas vesicles, mixotrophy, and so on) would help to confirm some of the potential mechanisms hypothesized for top-down and bottom-up control of vertical distributions. However, we note that the microscopy data in our study generally agreed with the FluoroProbe depth profiles, with the relative abundance of taxa identified in each lake by microscopy corresponding to that of spectral groups identified by the probe (Table S3).

Finally, our study addresses how top-down and bottom-up control of vertical distributions vary across a wide variety of north temperate lakes, but does not address how these controls may vary across time in a single lake. As such, we were able to relate top-down and bottom-up control to the characteristics of DCM across a gradient of lakes, but were not able to examine controls on the formation of DCM over time. Consideration of how seasonal dynamics affect top-down and bottom-up control of phytoplankton vertical distributions in a single lake or several similar lakes over time could elucidate the relative contribution of thermal stratification vs. lake depth as a bottom-up control of phytoplankton peak

formation. Such a study might also permit more intensive sampling of fewer study lakes, including collection of depth profiles of variables such as nutrients or grab samples of phytoplankton at specific depths, neither of which were available in our dataset. Finally, while our findings support findings using total Chl *a* data from other lakes globally (Leach et al. 2018), it would be beneficial to test our hypotheses regarding different phytoplankton spectral groups in lakes outside the north temperate zone.

Conclusions

Our research provides new insight on top-down and bottom-up control of phytoplankton biomass by extending this framework to the vertical distribution of both total phytoplankton and individual phytoplankton spectral groups. We hypothesized that the relative importance of top-down and bottom-up drivers could be related to the characteristics of phytoplankton taxa comprising each spectral group. We found that while phytoplankton biomass was driven by nutrient concentrations, the vertical distribution of phytoplankton was determined by both top-down and bottom-up controls, and that bottom-up control occurred via multiple mechanisms (light, thermal stratification, and nutrients). Moreover, the drivers of total biomass vertical distributions were not always the same as drivers of spectral group distributions, indicating that consideration of total biomass alone can mask responses of phytoplankton sub-groups to top-down and bottom-up controls.

Our data suggest that spectral group vertical distributions could be linked to functional traits of the phytoplankton taxa within each spectral group. Specifically, the vertical distributions of highly edible taxa such as chrysophytes and cryptophytes exhibited deeper, broader peaks when zooplankton were abundant, possibly due to greater grazing pressure. We also found that thermal stratification led to shallower, narrower peaks of cyanobacterial taxa that can regulate their buoyancy. Furthermore, light attenuation led to broader peak width in the green algae spectral group, possibly due to divergent responses to high light attenuation between mixotrophic and non-mixotrophic green algae. Finally, spectral groups were most divergent in their distributions when thermal stratification was high and light attenuation was low, permitting separation of spectral groups into distinct locations within the water column. Our study demonstrates that consideration of multiple phytoplankton groups and phytoplankton functional traits can help elucidate drivers of DCM characteristics and inform our understanding of the relative importance of top-down and bottom-up control in aquatic ecosystems.

References

Abbott, M. R., K. L. Denman, T. M. Powell, P. J. Richerson, R. C. Richards, and C. R. Goldman. 1984. Mixing and the dynamics of the deep chlorophyll maximum in Lake Tahoe. Limnol. Oceanogr. **29**: 862–78. doi:10.4319/lo.1984.29.4.0862

Albers, S., L. Winslow, D. Collinge, J. Read, T. Leach, and J. Zwart. 2018. rLakeAnalyzer: Lake physics tools. doi:10.5281/zenodo.1198428

Alldredge, A. L., T. J. Cowles, S. MacIntyre, et al. 2002. Occurrence and mechanisms of formation of a dramatic thin layer of marine snow in a shallow Pacific fjord. Mar. Ecol. Prog. Ser. **233**: 1–12. doi:10.3354/meps233001

Arvola, L., K. Salonen, P. Kankaala, and A. Lehtovaara. 1992. Vertical distributions of bacteria and algae in a steeply stratified humic lake under high grazing pressure from *Daphnia longispina*. Hydrobiologia **229**: 253–69. doi:10.1007/BF00007004

Barbiero, R. P., and C. M. McNair. 1996. The dynamics of vertical chlorophyll distribution in an oligomesotrophic lake. J. Plankton Res. **18**: 225–37. doi:10.1093/plankt/18.2.225

Beisner, B. E., and M. L. Longhi. 2013. Spatial overlap in lake phytoplankton: Relations with environmental factors and consequences for diversity. Limnol. Oceanogr. **58**: 1419–30. doi:10.4319/lo.2013.58.4.1419

Benndorf, J., W. Boing, J. Koop, and I. Neubauer. 2002. Top-down control of phytoplankton: The role of time scale, lake depth and trophic state. Freshw. Biol. **47**: 2282–95. doi:10.1046/j.1365-2427.2002.00989.x

Beutler, M., K. H. Wiltshire, B. Meyer, C. Moldaenke, C. Lüring, M. Meyerhöfer, U. P. Hansen, and H. Dau. 2002. A fluorometric method for the differentiation of algal populations in vivo and in situ. Photosynth. Res. **72**: 39–53. doi:10.1023/A:1016026607048

Breiman, L., J. H. Friedman, R. A. Olshen, and C. J. Stone. 1984. Classification and regression trees. *In* J. Kimmel, A. Cava, and J. Greenblatt [eds.], 1st ed. Wadsworth, Inc.

Brett, M. T., D. C. Müller-Navarra, A. P. Ballantyne, J. L. Ravet, and C. R. Goldman. 2006. Daphnia fatty acid composition reflects that of their diet. Limnol. Oceanogr. **51**: 2428–37. doi:10.4319/lo.2006.51.5.2428

Brett, M. T., D. C. Muller-Navarra, and S.-K. Park. 2000. Empirical analysis of the effect of phosphorus limitation on algal food quality for freshwater zooplankton. Limnol. Oceanogr. **45**: 1564–75. doi:10.4319/lo.2000.45.7.1564

Bunnell, D. B., R. P. Barbiero, S. A. Ludsin, and others. 2014. Changing ecosystem dynamics in the Laurentian Great Lakes: Bottom-up and top-down regulation. Bioscience **64**: 25–39. doi:10.1093/biosci/bit001

Camacho, A., E. Vicente, and M. R. Miracle. 2001. Ecology of Cryptomonas at the chemocline of a karstic sulfate-rich lake. Mar. Freshw. Res. **52**: 805–15. doi:10.1071/MF00097

Catherine, A., N. Escoffier, A. Belhocine, A. B. Nasri, S. Hamlaoui, C. Yéprémian, C. Bernard, and M. Troussellier. 2012. On the use of the FluoroProbe®, a phytoplankton quantification method based on fluorescence excitation spectra for large-scale surveys of lakes and

reservoirs. Water Res. **46**: 1771–84. doi:10.1016/j.watres.2011.12.056

Christensen, D. L., S. R. Carpenter, and K. L. Cottingham. 1995. Predicting chlorophyll vertical distribution in response to epilimnetic nutrient enrichment in small stratified lakes. J. Plankton Res. **17**: 1461–77. doi:10.1093/plankt/17.7.1461

Clegg, M. R., S. C. Maberly, and R. I. Jones. 2004. Dominance and compromise in freshwater phytoplanktonic flagellates: The interaction of behavioural preferences for conflicting environmental gradients. Funct. Ecol. **18**: 371–80. doi:10.1111/j.0269-8463.2004.00834.x

Clegg, M. R., S. C. Maberly, and R. I. Jones. 2007. Behavioral response as a predictor of seasonal depth distribution and vertical niche separation in freshwater phytoplanktonic flagellates. Limnol. Oceanogr. **52**: 441–55. doi:10.4319/lo.2007.52.1.0441

Cramer, M., and J. Myers. 1952. Growth and photosynthetic characteristics of *Euglena gracilis*. Arch. Mikrobiol. **17**: 384–402.

Cullen, J. J. 2015. Subsurface chlorophyll maximum layers: Enduring enigma or mystery solved? Ann. Rev. Mar. Sci. **7**: 207–39. doi:10.1146/annurev-marine-010213-135111

De'ath, G., and K. E. Fabricius. 2000. Classification and regression trees: A powerful yet simple technique for ecological data analysis. Ecology **81**: 3178–92. doi:10.1890/0012-9658(2000)081[3178:CARTAP]2.0.CO;2

deNoyelles Jr, F., V. H. Smith, J. H. Kastens, and others. 2016. A 21-year record of vertically migrating subepilimnetic populations of Cryptomonas spp. Inl. Waters **6**: 172–184. doi:10.5268/IW-6.2.930

Derks, A., K. Schaven, and D. Bruce. 2015. Diverse mechanisms for photoprotection in photosynthesis. Dynamic regulation of photosystem II excitation in response to rapid environmental change. Biochim. Biophys. Acta Bioenerg. **1847**: 468–85. doi:10.1016/j.bbabio.2015.02.008

Du, X., E. Garcia-Berthou, Q. Wang, J. Liu, T. Zhang, and Z. Li. 2015. Analyzing the importance of top-down and bottom-up controls in food webs of Chinese lakes through structural equation modeling. Aquat. Ecol. **49**: 199–210. doi:10.1007/s10452-015-9518-3

Durham, W. M., and R. Stocker. 2011. Thin phytoplankton layers: Characteristics, mechanisms, and consequences. Ann. Rev. Mar. Sci. **4**: 177–207. doi:10.1146/annurev-marine-120710-100957

Ellis, B. K., J. A. Stanford, D. Goodman, and others. 2011. Long-term effects of a trophic cascade in a large lake ecosystem. Proc. Natl. Acad. Sci. **108**: 1070–1075. doi:10.1073/pnas.1013006108

Fee, E. J. 1976. The vertical and seasonal distribution of chlorophyll in lakes of the experimental lakes area, northwestern Ontario: Implications for primary production estimates. Limnol. Oceanogr. **21**: 767–83. doi:10.4319/lo.1976.21.6.0767

Fennel, K., and E. Boss. 2003. Subsurface maxima of phytoplankton and chlorophyll: Steady-state solutions from a simple model. Limnol. Oceanogr. **48**: 1521–34. doi:10.4319/lo.2003.48.4.1521

Ghadouani, A., and R. E. H. Smith. 2005. Phytoplankton distribution in Lake Erie as assessed by a new in situ spectrofluorometric technique. J. Great Lakes Res. **31**:154–67. doi:10.1016/S0380-1330(05)70311-7

Gregor, J., and B. Maršálek. 2004. Freshwater phytoplankton quantification by chlorophyll a: A comparative study of in vitro, in vivo and in situ methods. Water Res. **38**: 517–22. doi:10.1016/j.watres.2003.10.033

Hamilton, D. P., K. R. O. Brien, and C. G. Mcbride. 2010. Vertical distributions of chlorophyll in deep, warm monomictic lakes. Aquat. Sci. **72**: 295–307. doi:10.1007/s00027-010-0131-1

Hamre, K. D., A. B. Gerling, Z. W. Munger, J. P. Doubek, R. P. McClure, K. L. Cottingham, and C. C. Carey. 2017. Spatial variation in dinoflagellate recruitment along a reservoir ecosystem continuum. J. Plankton Res. **39**: 715–28. doi:10.1093/plankt/fbx004

Hamre, K., M. E. Lofton, R. McClure, Z. Munger, J. Doubek, A. Gerling, M. Schreiber, and C. Carey. 2018. In situ fluorometry reveals a persistent, perennial hypolimnetic cyanobacterial bloom in a seasonally anoxic reservoir. Freshw. Sci. **37**: 483–95. doi:10.1086/699327

Hansson, T. H., H.-P. Grossart, P. A. del Giorgio, N. F. St-Gelais, and B. E. Beisner. 2019. Environmental drivers of mixotrophs in boreal lakes. Limnol. Oceanogr. **64**: 1688–1705. doi:10.1002/lno.11144

Harper, E. B., J. C. Stella, and A. K. Fremier. 2011. Global sensitivity analysis for complex ecological models: A case study of riparian cottonwood population dynamics. Ecol. Appl. **21**: 1225–40. doi:10.1890/10-0506.1

Hillebrand, H., C.-D. Dürselen, D. Kirschtel, U. Pollingher, and T. Zohary. 1999. Biovolume calculation for pelagic and benthic microalgae. J. Phycol. **35**: 403–24. doi:10.1046/j.1529-8817.1999.3520403.x

Holm, N. P., G. G. Ganf, and J. Shapiro. 1983. Feeding and assimilation rates of *Daphnia pulex* fed *Aphanizomenon flos-aquae*. Limnol. Oceanogr. **28**: 677–87. doi:10.4319/lo.1983.28.4.0677

Jeppesen, E., J. P. Jensen, C. Jensen, B. Faafeng, D. O. Hessen, M. Søndergaard, and T. Lauridsen. 2003. The impact of nutrient state and lake depth on top-down control in the pelagic zone of lakes: A study of 466 lakes from the temperate zone to the arctic. Ecosystems **6**: 313–25. doi:10.1007/s10021-002-0145-1

Karpowicz, M., and J. Ejsmont-Karabin. 2017. Effect of metalimnetic gradient on phytoplankton and zooplankton (Rotifera, Crustacea) communities in different trophic conditions. Environ. Monit. Assess. **189**: 1–13. doi:10.1007/s10661-017-6055-7

Kirk, J. T. O. 2011. Light and photosynthesis in aquatic ecosystems, 3rd Edition. Cambridge Univ. Press.

Klausmeier, A., and E. Litchman. 2001. Algal games: The vertical distribution of phytoplankton in poorly mixed water columns. Limnol. Oceanogr. **46**: 1998–2007. doi:10.4319/lo.2001.46.8.1998

Kononen, K., and others. 2003. Development of a deep chlorophyll maximum of *Heterocapsa triquetra* Ehrenb. at the entrance to the Gulf of Finland. Limnol. Oceanogr. **48**: 594–607. doi:10.4319/lo.2003.48.2.0594

Kring, S. A., S. E. Figary, G. L. Boyer, S. B. Watson, and M. R. Twiss. 2014. Rapid in situ measures of phytoplankton communities using the bbe FluoroProbe: Evaluation of spectral calibration, instrument intercompatibility, and performance range. Can. J. Fish. Aquat. Sci. **71**: 1087–95. doi:10.1139/cjfas-2013-0599

Lampert, W., W. Fleckner, H. Rai, and B. E. Taylor. 1986. Phytoplankton control by grazing zooplankton: A study on the spring clear-water phase. Limnol. Oceanogr. **31**: 478–90. doi:10.4319/lo.1986.31.3.0478

Latasa, M., A. M. Cabello, X. A. G. Morán, R. Massana, and R. Scharek. 2017. Distribution of phytoplankton groups within the deep chlorophyll maximum. Limnol. Oceanogr. **62**: 665–85. doi:10.1002/lno.10452

Leach, T. H., B. E. Beisner, C. C. Carey, and others. 2018. Patterns and drivers of deep chlorophyll maxima structure in 100 lakes: The relative importance of light and thermal stratification. Limnol. Oceanogr. **63**: 628–646. doi:10.1002/lno.10656

Lewis, D. M., A. Brereton, and J. T. Siddons. 2017. A large eddy simulation study of the formation of deep chlorophyll/biological maxima in un-stratified mixed layers: The roles of turbulent mixing and predation pressure. Limnol. Oceanogr. **62**: 2277–307. doi:10.1002/lno.10566

Longhi, M. L., and B. E. Beisner. 2009. Environmental factors controlling the vertical distribution of phytoplankton in lakes. J. Plankton Res. **31**: 1195–207. doi:10.1093/plankt/fbp065

Lynch, M., and J. Shapiro. 1981. Predation, enrichment, and phytoplankton community structure. Limnol. Oceanogr. **26**: 86–102. doi:10.4319/lo.1981.26.1.0086

Margalef, R. 1983. Limnologia. Ediciones Omega.

McCauley, E. 1984. The estimation of the abundance and biomass of zooplankton in samples. In A manual on methods for the assessment of secondary productivity in fresh waters. Blackwell Scientific, 228–65.

McQueen, D. J., M. R. S. Johannes, J. R. Post, T. J. Stewart, and D. R. S. Lean. 1989. Bottom-up and top-down impacts on freshwater pelagic community structure. Ecol. Monogr. **59**: 289–309. doi:10.2307/1942603

Medrano, E. A., R. E. Uittenbogaard, B. J. H. Van De Wiel, L. M. D. Pires, and H. J. H. Clercx. 2016. An alternative explanation for cyanobacterial scum formation and persistence by oxygenic photosynthesis. Harmful Algae **60**: 27–35. doi:10.1016/j.hal.2016.10.002

Moeller, H. V., C. Laufkötter, E. M. Sweeney, and M. D. Johnson. 2019. Light-dependent grazing can drive formation and deepening of deep chlorophyll maxima. Nat. Commun. **10**: 1978. doi:10.1038/s41467-019-09591-2

Moll, R. A., M. Z. Brahce, and T. P. Peterson. 1984. Phytoplankton dynamics within the subsurface chlorophyll maximum of Lake Michigan. J. Plankton Res. **6**: 751–66. doi:10.1093/plankt/6.5.751

Oliver, R. L. 1994. Floating and sinking in gas-vacuolate cyanobacteria. J. Phycol. **30**: 161–73. doi:10.1111/j.0022-3646.1994.00161.x

Pilati, A., and W. A. Wurtsbaugh. 2003. Importance of zooplankton for the persistence of a deep chlorophyll layer: A limnocorral experiment. Limnol. Oceanogr. **48**: 249–60. doi:10.4319/lo.2003.48.1.0249

Read, J., D. Hamilton, I. D. Jones, K. Muraoka, L. Winslow, R. Kroiss, C. Wu, and E. Gaiser. 2011. Derivation of lake mixing and stratification indices from high-resolution lake buoy data. Environ. Model. Software **26**: 1325–36. doi:10.1016/j.envsoft.2011.05.006

Ryabov, A. B., and B. Blasius. 2014. Depth of the biomass maximum affects the rules of resource competition in a water column. Am. Nat. **184**: E132–46. doi:10.1086/677544

Sawatzky, C. L., W. A. Wurtsbaugh, and C. Luecke. 2006. The spatial and temporal dynamics of deep chlorophyll layers in high-mountain lakes: Effects of nutrients, grazing and herbivore nutrient recycling as growth determinants. J. Plankton Res. **28**: 65–86. doi:10.1093/plankt/fbi101

Selmeczy, G. B., K. Tapolczai, P. Casper, L. Krienitz, and J. Padisák. 2016. Spatial- and niche segregation of DCM-forming cyanobacteria in Lake Stechlin (Germany). Hydrobiologia **764**: 229–40. doi:10.1007/s10750-015-2282-5

Sengupta, A., F. Carrara, and R. Stocker. 2017. Phytoplankton can actively diversify their migration strategy in response to turbulent cues. Nature **543**: 555–8. doi:10.1038/nature21415

Shapiro, J. 1973. Blue-green algae: Why they become dominant. Science **179**: 382–4. doi:10.1126/science.179.4071.382

Taylor, J. M., M. J. Vanni, and A. S. Flecker. 2015. Top-down and bottom-up interactions in freshwater ecosystems: Emerging complexities. In Trophic ecology: Bottom-up and top-down interactions across aquatic and terrestrial ecosystems. Cambridge Univ. Press, 55–85.

Therneau, T., and B. Atkinson. 2019. Rpart: Recursive partitioning and regression trees. v. 4.1-15. https://cran.r-project.org/web/packages/rpart/index.html.

Tittel, J., V. Bissinger, U. Gaedke, and N. Kamjunke. 2005. Inorganic carbon limitation and mixotrophic growth in

Chlamydomonas from an acidic mining lake. Protist **156**: 63–75. doi:10.1016/j.protis.2004.09.001

Varela, R. A., A. Cruzado, and J. Tintoré. 1994. A simulation analysis of various biological and physical factors influencing the deep-chlorophyll maximum structure in oligotrophic areas. J. Mar. Syst. **5**: 143–57. doi:10.1016/0924-7963(94)90028-0

Visser, P. M., J. Passarge, and L. R. Mur. 1997. Modelling vertical migration of the cyanobacterium microcystis. Hydrobiologia **349**: 99–109. doi:10.1023/A:1003001713560

Yang, S., W. Jin, S. Wang, X. Hao, Y. Yan, M. Zhang, and B. Zheng. 2015. Chlorophyll ratio analysis of the responses of algae communities to light intensity in spring and summer in Lake Erhai. Environ. Earth Sci. **74**: 3877–85. doi:10.1007/s12665-015-4140-1

Yoshiyama, K., J. P. Mellard, E. Litchman, and C. A. Klausmeier. 2009. Phytoplankton competition for nutrients and light in a stratified water column. Am. Nat. **174**: 190–203. doi:10.1086/600113

Yuan, L. L., and A. I. Pollard. 2018. Changes in the relationship between zooplankton and phytoplankton biomasses across a eutrophication gradient. Limnol. Oceanogr. **63**: 2493–507. doi:10.1002/lno.10955

Acknowledgments

The study was developed in collaboration by all authors. B.E.B. provided data for the 51 study lakes and code for calculating spatial overlap, and T.H.L. provided code for peak curve-fitting calculations. M.E.L. conducted all analyses, developed all figures, and drafted the manuscript with continuous feedback on the scope and analysis by C.C.C. All authors worked together to interpret results, provide feedback on the manuscript, and approved its final version. We thank Maria Longhi and Allain Barnett for data collection. Bryan Brown, Erin Hotchkiss, the Carey Lab at Virginia Tech, Global Lakes Ecological Observatory Network collaborators, and the Pacific Rim Applications and Grid Middleware Assembly Lake Expedition team provided helpful feedback. NSF 1737424, 1753639, 1702506, and 1234983 to C.C.C.; Natural Sciences and Engineering Research Council (NSERC) and Fonds de recherche du Québec - nature et technologie (FRQNT) funding to B.E.B.; Virginia Tech William R. Walker Graduate Research Fellow Award and Virginia Lakes and Watersheds Association Leo Bourassa Scholarship to M.E.L.

Conflict of Interest

None declared.

Submitted 24 August 2019
Revised 11 February 2020
Accepted 20 April 2020

Associate editor: Susanne Menden-Deuer